Materials Chemistry and Physics, 18 (1987) 81–92

THE TRAPPING OF Gd^{3+} EXCITATION ENERGY BY Cr^{3+} AND RARE EARTH IONS IN $GdAlO_3$

A.J. DE VRIES, W.J.J. SMEETS and G. BLASSE

Physical Laboratory, State University Utrecht, P.O. Box 80.000,
3508 TA Utrecht (The Netherlands)

Received February 18, 1987; accepted March 12, 1987

ABSTRACT

The trapping of Gd^{3+} excitation energy by several activator ions in $GdAlO_3$ is reported. The activator ions are Cr^{3+}, Sm^{3+}, Eu^{3+}, Tb^{3+}, Dy^{3+} Er^{3+} and Tm^{3+}. If a broad, allowed absorption band of the activator overlaps with the ^6I or ^6P levels of Gd^{3+}, efficient trapping is possible via multipolar interaction (trapping rate $10^{6\pm1}s^{-1}$). Exchange interaction is responsible for trapping by rare-earth ions without such allowed absorption bands (trapping rate $10^{3\pm1}s^{-1}$). At very low temperatures Gd^{3+} traps can act as efficient trapping centres, resulting in Gd^{3+} trap emission. The emission of Fe^{3+} on octahedral sites is also reported.

INTRODUCTION

During recent years the energy transfer and energy migration processes in Gd^{3+} compounds have been of considerable interest. In several papers the reasons for this have been indicated [1-3]. These compounds are challenging not only from a fundamental point of view, but also in view of their potential use as, for example, phosphors in fluorescent lamps.

For Gd^{3+} compounds which yield a high luminescence efficiency upon short-wavelength UV-excitation, three processes can be indicated which influence the luminescence efficiency.

i) The sensitization of the Gd^{3+} sublattice by a sensitizer ion
ii) The energy migration among the Gd^{3+} ions
iii) The trapping of the migrating excitation energy by activator ions.

0254-0584/87/$3.50

Much attention has been paid to the first two processes [4-8]. The aim of this paper is the study of the trapping by several, different activator ions in $GdAlO_3$, in particular to determine the factors influencing the trapping efficiency. The $GdAlO_3$ lattice was chosen for this investigation in view of the simple arrangement of the Gd^{3+} ions (a three-dimensional, approximate s.c. Gd^{3+} sublattice [9]) and the possibility to introduce rare earth ions on the Gd^{3+} sites, as well as transition metal ions on the Al^{3+} sites.

The compositions $GdAlO_3$-1%X (with X= Cr^{3+}, Sm^{3+}, Eu^{3+}, Tb^{3+}, Dy^{3+}, Er^{3+}, Tm^{3+}) were investigated. We also tried to incorporate Fe^{3+} in $GdAlO_3$, but it turned out that iron was incorporated with different valencies.

EXPERIMENTAL

Powder samples of $GdAlO_3$-1%X (with X = Cr^{3+}, Fe^{3+}, Sm^{3+}, Eu^{3+}, Tb^{3+}, Dy^{3+}, Er^{3+} and Tm^{3+}) were prepared by usual solid state techniques, with starting materials Sm_2O_3, Eu_2O_3, Gd_2O_3, Tb_4O_7, Dy_2O_3, Er_2O_3, Tm_2O_3 (all Highways Int. 99.999%), $Al(NO_3)_3.9H_2O$ (Merck, p.a.). Cr_2O_3(B.D.H.) and Fe_2O_3(Baker). The final firing procedure was performed at 1430°C. The samples were checked by X-ray powder diffraction. The luminescence measurements were performed on a Perkin-Elmer MPF-3L spectrofluorometer equipped with an Oxford instruments CF-100 helium flow cryostate. The spectra were corrected for photomultiplier response and for lamp output.

RESULTS

The relative trapping efficiency in the different samples was determined by measuring the emission intensity between 300 and 800 nm after excitation in the Gd^{3+} ^6I levels. In view of the low absorption strength of the $^8S \rightarrow {}^6P$ transitions, we were not able te perform this study with reasonable accuracy after excitation in the ^6P levels. The total activator emission, is a qualitative measure for the trapping efficiency. In this way the sequence found for the trapping efficiency of the different ions is:$Er^{3+} < Tm^{3+} < Dy^{3+} < Sm^{3+} < Eu^{3+} \approx Tb^{3+} < Cr^{3+}$.

Apart from the emission of the activator ion, in some samples also Gd^{3+} and Cr^{3+} emission was observed upon excitation in Gd^{3+} (^6I). This Cr^{3+} emission must be due to the presence of a small amount of Cr^{3+} in the starting material $Al(NO_3)_3.9H_2O$($\approx$ 10 ppm). In Table I data are presented on the presence of the Gd^{3+} (^6P) and Cr^{3+} emission at 4.2 K and 298 K upon excitation of the Gd^{3+} ions (^6I) of samples to which no Cr^{3+} was intentionally added.

For all samples the excitation spectrum of the activator emission was measured. In Figs. 1 and 2, two representative examples are presented, viz. for Cr^{3+} and Tb^{3+}. The assignment of the different excitation features is given in the figures.

The broad band between 34.000 and 38.000 cm^{-1} in the excitation spectrum of the Tb^{3+} emission is assigned to the spin-forbidden component of the $4f^8$-$4f^75d$ transition of Tb^{3+}, in view of its low absorption strength.

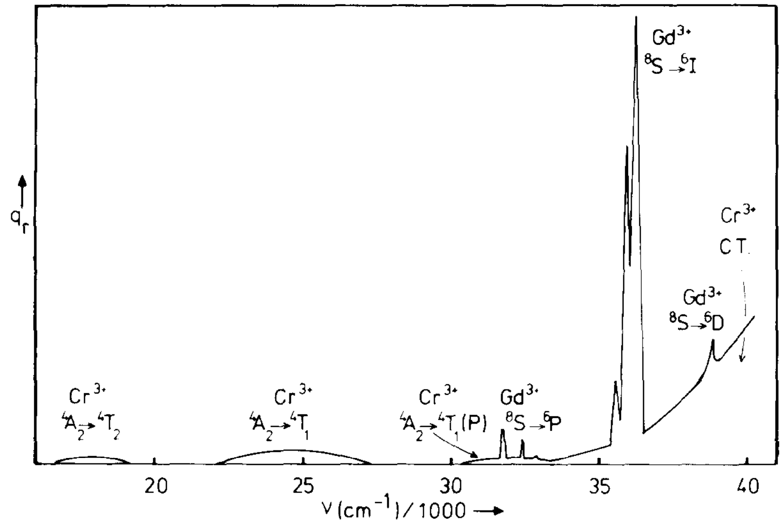

Fig. 1. Excitation spectrum of the Cr^{3+} emission at 13.750 cm^{-1} in $GdAlO_3$-1% Cr^{3+} at 298 K; q_R gives the relative quantum output in arbitrary units.

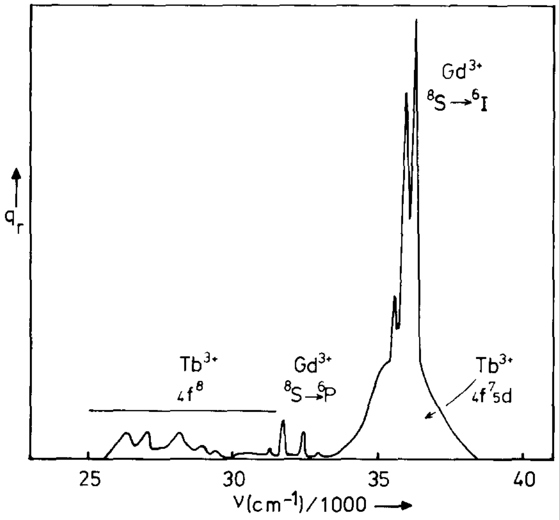

Fig. 2. Excitation spectrum of the Tb^{3+} emission at 18.350 cm^{-1} in $GdAlO_3$-1%Tb^{3+} at 298K; q_R gives the relative quantum output in arbitrary units.

The excitation spectrum of the Eu^{3+} emission shows in addition to the characteristic transitions within the $4f^6$ configuration of Eu^{3+} and the Gd^{3+} lines, a broad band with a maximum at 38.000 cm^{-1} which is due to a charge-transfer transition [10].

The excitation spectra of the other activator ions show also the Gd^{3+} levels, although these lines, especially in the case of Er^{3+} and Tm^{3+} are less pronounced compared to the lines of the activator ions than in the case of, for example, Tb^{3+}. In Fig. 3 the ratio between the intensity of the $^8S \rightarrow {}^6I$ and $^8S \rightarrow {}^6P$ transitions of Gd^{3+} in the excitation spectra of the activator ions is presented. This ratio is used to determine whether the ^6I or the ^6P levels of Gd^{3+} are involved in the trapping of the excitation energy by the activator ion. (see discussion)

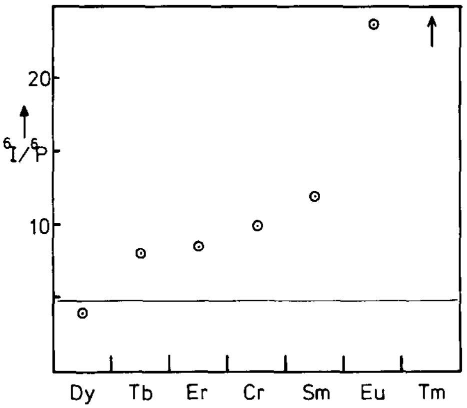

Fig. 3. Intensity ratio of a $^8S \rightarrow {}^6I$ and a $^8S \rightarrow {}^6P$ Gd^{3+} line in the excitation spectra of the activator emission. The drawn line gives this ratio found for the diffuse reflection spectrum of $GdAlO_3$. For Tm^{3+} this ratio is larger than 25.

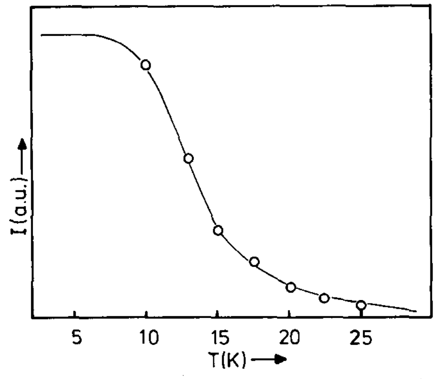

Fig. 4. Temperature dependence of the Gd^{3+} trap emission in $GdAlO_3$-1%Tb^{3+}. The drawn line is the fitcurve for this temperature dependence (see text).

The Gd^{3+} emission shows a strong temperature dependence at low temperatures. In Fig. 4 the temperature dependence at low temperatures of the Gd^{3+} emission in $GdAlO_3$-Tb^{3+} is presented. The Gd^{3+} emission at low temperatures is at lower energy than the Gd^{3+} emission at room temperature. This has been observed before in other Gd^{3+} compounds [3,11,12]. The emission at low temperatures is assigned to emission from Gd^{3+} traps (i.e. Gd^{3+} ions on perturbed sites, e.g. Gd^{3+} at Al^{3+} sites). Since the used instrumentation does not have a high resolving power (> 0.5 nm at 300 nm), the trap emission observed may well be an average of different trap emissions. The trap depth can be calculated using the temperature dependence of the trap emission [11]. From the temperature dependence of the trap emission in the different samples a trap depth of 50 cm^{-1} could be derived. Because the emission of the intrinsic Gd^{3+} ions was too weak to determine accurately the position of this emission, it was not possible to calculate this trap depth from the spectroscopic data.

In some samples a weak emission is observed between 13.500 and 14.500 cm^{-1} (Fig. 5). It shows a considerable amount of structure. The emission intensity decreases upon increasing the temperature. The excitation spectrum of this emission consists of a broad band with its maximum around 30.300 cm^{-1}.

This emission with a decay time of approximately 2.2 ms at 200 K is assigned to emission from a Fe^{3+} ion at an octahedral site. (see also discussion). The ion is also present in the starting $Al(NO_3)_3 \cdot 9H_2O$ (≈ 20 ppm).

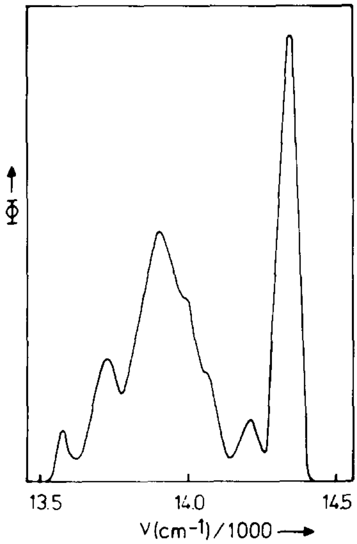

Fig. 5. Emission spectrum of the Fe^{3+} luminescence after excitation at 30.300 cm^{-1} in $GdAlO_3$-Cr^{3+} at 4.2K. Φ gives the spectral radiant power per constant energy interval in arbitrary units.

Samples intentionally doped with Fe^{3+} behaved similarly. It was not possible to excite the Fe^{3+} emission in the Gd^{3+} ion. Another transition metal ion which showed up sometimes was Mn^{2+} with a broad emission band with a maximum around 16.600 cm^{-1}. The excitation spectrum of this emission showed a band with a maximum around 29.400 cm^{-1}.

DISCUSSION

Rates in the Gd^{3+} sublattice

The processes, which can occur after excitation of the ^6I level of Gd^{3+} in a concentrated Gd^{3+} system, are schematically given in Fig. 6.

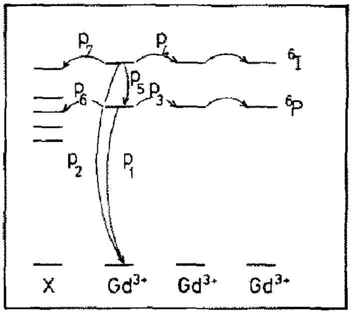

Fig. 6. Processes which occur after excitation of the ^6I level of Gd^{3+} in a concentrated Gd^{3+} system.
p_1: radiative decay from ^6P
p_2: radiative decay from ^6I
p_3: transfer of the excitation energy to another Gd^{3+} ion via the ^6P level
p_4: transfer of the excitation energy to another Gd^{3+} ion via the ^6I level
p_5: radiationless decay from the ^6I to the ^6P level
p_6: transfer of the excitation energy to an activator ion via the ^6P level
p_7: transfer of the excitation energy to an activator ion via the ^6I level.

We can estimate the probabilities of most of these processes (p_1-p_7) using data found in other compounds. The radiative rate p_1 is estimated to be $10^2 s^{-1}$ [3,11,12]. In view of the higher absorption strength of the $^8S \rightarrow {}^6I$ transition ([13] Figs 1+2) the value of p_2 is estimated to be $10^3 s^{-1}$.

The values of P_3 and P_4 will not differ much, especially since exchange interaction seems to play a dominating role in the Gd-Gd transfer [8]. In case of energy migration over the Gd^{3+} sublattice in the rapid transfer regime, which may be the case here due to the short (3.8Å) distance between neighbouring Gd^{3+} ions, the Gd^{3+}-Gd^{3+} transfer probability is approximately $10^{7\pm1} s^{-1}$ [7]. The probability for radiationless decay from the ^6I level to the ^6P level of Gd^{3+} can be estimated using the experimental energy gap law, which was modified by Van Dijk and Schuurmans [14]:

$$k_{nr} = \beta_{el} \exp[-(\Delta E_0 - 2\hbar\omega_{max})\alpha]$$

where α and β_{el} are constants, ΔE_o is the energy gap between the $4f^7$ levels involved and ω_{max} is the highest frequency mode of the host lattice. With α = $4.6*10^{-3}$cm, $\beta_{el}=4*10^7 s^{-1}$, ΔE_o = 2500 cm^{-1} and $\hbar\omega_{max}$=600 cm^{-1}, the probability for the radiationless decay from the ^6I to the ^6P levels has a value p_5 = $10^5 s^{-1}$.

The values of p_6 and p_7 depend on the nature of the activator ion and the interaction process between the Gd^{3+} ion and the activator ion.

Because $p_4 \gg p_5 \gg p_2$ (and $p_3 \gg p_1$), it is possible that after excitation into the ^6I levels of Gd^{3+}, the energy migrates over the Gd^{3+} sublattice via the ^6I levels for some time. Migration over the ^6I levels of Gd^{3+} was suggested before in other Gd^{3+} compounds [16]. Since p_4 = $100(p_5+p_2)$, the excitation energy will migrate about 100 steps over the ^6I levels before relaxation to the ^6P levels occurs. During these 100 steps the excitation energy may be trapped by an activator ion. This depends on the value of p_7. After relaxation to the ^6P levels, the energy migrates over the ^6P levels. The number of steps during the lifetime of the excited state will be much larger for Gd^{3+} in this level, viz ≈ 10^5 ($=p_3/p_1$). During this migration the excitation energy may be trapped by an activator (or killer).

Trapping rate

The ratio of the $^8S \rightarrow {}^6I$ and $^8S \rightarrow {}^6P$ lines of the Gd^{3+} ion in the excitation spectrum of the activator emission contains information about the relative magnitudes of p_6 and p_7. If $p_7 \leqslant p_6$, the lines are expected to have the same intensity ratio as in the diffuse reflection spectrum. This is the case for all the activator ions except Tm^{3+} and Eu^{3+} (see Fig. 3). This ratio is expected to be larger than in the diffuse reflection spectrum if the total transfer process to the activator has a higher probability via the ^6I than via the ^6P levels. This is the case for Eu^{3+} and Tm^{3+}.

Not only the ratio between p_6 and p_7 will depend on the choice of the activator ion, but also the series of values of p_6 and those of p_7. The difference in these values accounts for the difference in the trapping efficiency of the activator ions.

The sequence found for this efficiency from the intensity of the activator ion emission, is supported further by the occurrence of Cr^{3+} and Gd^{3+} emission after excitation in the Gd^{3+} ^6I levels (see Table I). If the trapping by the activator ion is not very efficient, trapping by other ions (e.g. impurity ions) can occur. Consequently, the presence of Gd^{3+} emission and Cr^{3+} emission points to a low trapping rate. The intensity of these emissions compared to the emission of the activator ion gives a qualitative indication of this trapping rate.

Table I. Presence of Gd^{3+} and Cr^{3+} emission in $GdAlO_3$-1%X upon excitation in $Gd^{3+}(^6I)$ at 4.2 K and 298 K.

	4.2 K		298 K	
X	Gd^{3+} emission	Cr^{3+} emission	Gd^{3+} emission	Cr^{3+} emission
Eu^{3+}	0	-	-	-
Tb^{3+}	0	-	-	-
Sm^{3+}	0	+	0	+
Dy^{3+}	+	+	0	+
Tm^{3+}	+	+	0	+
Er^{3+}	+	+	+	+

-: not present; 0: present, but weak; +: clearly present

The highest trapping rates are found for Cr^{3+}, Eu^{3+} and Tb^{3+}. Cr^{3+} and Eu^{3+} have broad excitation bands which overlap the Gd^{3+} ^6I and ^6P levels. For Cr^{3+} the $^4A_2$ - $^4T_1$ (P) excitation band overlaps with the ^6P levels and the change transfer excitation band overlaps with the ^6I levels. From the spectral overlap between the Gd^{3+} levels and the Cr^{3+} excitation bands and assuming electric-dipole interaction to be the main interaction mechanism in the Gd^{3+}-Cr^{3+} energy transfer, it is possible to calculate the ratio p_7/p_2 and p_6/p_1 using data and formulae from the literature [6,17]. In this way we find for both ratio's 10^3. This means that the values of p_7 and p_6 are $10^6 s^{-1}$ and $10^5 s^{-1}$, respectively. This means that trapping can occur via the ^6I and via the ^6P levels. This follows also from the excitation spectrum of the Cr^{3+} emission. For Eu^{3+} the situation is different. The Eu^{3+} charge-transfer band overlaps mainly with the ^6I levels of Gd^{3+}. The overlap with the ^6P levels of Gd^{3+} is small. For Eu^{3+} we find for the ratio p_7/p_2 and p_6/p_1 10^3 and 10, respectively. This yields for p_7 and p_6 $10^6 s^{-1}$ and $10^3 s^{-1}$, respectively. For Eu^{3+} p_7 is larger than p_5, and much larger than p_6, which means that most of the ^6I excitation energy is transfered from the ^6I levels to Eu^{3+}. The transfer from the ^6P levels to Eu^{3+} has a much lower probability. This is in accordance with the excitation spectrum of the Eu^{3+} emission.

The spinforbidden $4f^65d$ absorption band of Tb^{3+} overlaps also the ^6I levels of Gd^{3+}. If we calculate p_7 from the spectral overlap between this band and the Gd^{3+} ^6I levels we find $p_7 = 10^3 s^{-1}$. This value is smaller than p_5, which means that only a small part of the ^6I excitation energy is transfered from the ^6I levels of the Gd^{3+} to the Tb^{3+} ions via the $4f^65d$ state.

In this connection it is interesting to note that in $GdAlO_3$-Ce^{3+} extremely efficient transfer occurs from Gd^{3+} to Ce^{3+} [18]. The Gd^{3+} emission line peaks into the completely allowed 4f→5d absorption band of the Ce^{3+} ion, so that this transfer process is comparable to that of Cr^{3+} and Eu^{3+}. The values of p_6 and p_7 in case of Ce^{3+} are ~ $10^7 s^{-1}$ [18].

Table II. Oscillator strength of activator ion absorption lines around 32.100 cm^{-1} [13].

Activation ion	Oscillator strength
Er^{3+}	9.0×10^{-8}
Tb^{3+}	1.2×10^{-7}
Sm^{3+}	5.0×10^{-7}
Eu^{3+}	7.0×10^{-7}
Dy^{3+}	2.0×10^{-6}
Tm^{3+}	2.3×10^{-6}

The other activator ions do not have broad excitation bands near the Gd^{3+} levels. For Tb^{3+}, Sm^{3+}, Dy^{3+}, Er^{3+} and Tm^{3+} the trapping rate is determined by other factors. In the case of the host lattice Gd_2GeO_5 [19] evidence has been found that the trapping rate for rare earth ions was determined by the oscillator strength of the activator ion absorption lines near the Gd^{3+} ^6P levels, suggesting that the transfer occurs by multipole interaction. In Table II the oscillator strength of the activator ion absorption lines near the Gd^{3+} ^6P levels are given for aqueous solutions. This table shows that the sequence found for increasing trapping rate does not coïncide with the sequence in the oscillator strengths. Consequently the transfer process is not governed by multipole interaction. However, it is possible to explain the trapping sequence by assuming an exchange interaction due to an admixture of the X^{4+}-Gd^{2+} and/or X^{2+}-Gd^{4+} states (X = activator ion), the so called kinetic exchange [20]. Using the values of the standard reduction potentials as given by Carnall [21], it is possible to estimate the energy difference between the X^{3+}-Gd^{3+} state and the lower one of the X^{4+}-Gd^{2+} or the X^{2+}-Gd^{4+} states. Results are given in Table III. These values indicate the standard EMF of the reactions involved. The more negative this potential, the higher in energy lies the excited state concerned, and the lower the transfer probability for exchange interaction. This strongly suggests that in the host lattice $GdAlO_3$ exchange is the dominating mechanism in trapping in the case of activator ions without allowed transitions. This conclusion differs from that for Gd_2GeO_5 [19]. We ascribe this difference to the fact that the rare earth site in $GdAlO_3$ is near inversion symmetry, whereas that in Gd_2GeO_5 differs considerably from that symmetry. This restricts the forced electric-dipole oscillator strength for the former host.

Table III. Energy difference between the X^{4+}-Gd^{2+} state and the X^{3+}-Gd^{3+} state, characterized by the standard EMF values (see text).

Activation ion (=X)	standard EMF (V)
Tb^{3+}	-7.2
Eu^{3+}	-8.2^*
Dy^{3+}	-8.9
Sm^{3+}	-9.1
Tm^{3+}	-10.0^{**}
Er^{3+}	-10.0

* This value relates to the X^{2+}-Gd^{4+} state which has lower than the X^{4+}-Gd^{2+} state.

** This value relates to the X^{2+}-Gd^{4+} and the X^{4+}-Gd^{2+} state which have comparable energies.

The Tm^{3+} ion plays a special role as is clear from Fig. 3. This is due to the fact that the mismatch between the Gd^{3+} (^6P) level is several thousands cm^{-1}, so that p_6 vanishes. For the other ions the mismatch is one order of magnitude smaller; we assumed that it does not play a decisive role in the differences observed for the different activators.

The question arises what the values of p_6 and/or p_7 are for the exchange mediated process. A rough guess runs as follows: (i) the rare-earth emission is of the same order of magnitude as that of the Cr^{3+} impurity emission; (ii) the impurity concentration is a factor of about 10^3 lower than the rare-earth concentration; (iii) for multipolar trapping, like for Cr^{3+}, we found $P_{6,7} \sim 10^6 s^{-1}$; therefore $p_{6,7}$ is $10^{3\pm1}$ for the exchange-mediated trapping. Here the minus sign relates to Er^{3+}, the plus sign to Sm^{3+} and Dy^{3+}. The value for Tb^{3+} (no Cr^{3+} emission) lies higher, in good agreement with results observed elsewhere [11]. The estimation given is in line width the fact that also Gd^{3+} emission is observed in the case of a 1% doping level with Sm^{3+}, Dy^{3+}, Tm^{3+} or Eu^{3+}.

The Fe^{3+} emission

The Fe^{3+} emission observed in some samples (Fig. 5) is similar to one of the two Fe^{3+} emissions found in single-crystalline $LiAl_5O_8$ [22]. In single-crystalline $LiAl_5O_8$, the Fe^{3+} ion occupies both tetrahedral and octahedral sites. The Fe^{3+} ion at the octahedral site gives rise to an emission line at 14.300 cm^{-1} (with vibronic sidebands) with a corresponding excitation band with a maximum at 30.300 cm^{-1}. This emission has a decay time of 3.3 ms. Our emission has the same characteristics. In $GdAlO_3$ only octahedral sites are present for Fe^{3+}. The dominating vibronic sideband is at 430 cm^{-1}, indicating coupling with an Fe-O deproportional mode..

The excitation band is probably due to a charge-transfer transition [23]. Excitation bands due to transitions within the Fe^{3+} $3d^5$ configuration were not observed due to the low probability of transitions within this configuration and the low intensity of the Fe^{3+} emission. It is highly surprising that the Fe^{3+} emission cannot be excited into the Gd^{3+} levels. At least the $^6P \rightarrow {}^8S$ emission overlaps favourably with the Fe^{3+} charge-transfer band. The only possible explanation is the presence of Fe^{2+} which might be an effective killer. In this aspect it is interesting to note that the samples seem also to contain Mn^{2+} as is evident from some of the emission spectra. Recently Van Die *et al*. [24] have shown that in the related $LaAlO_3$-Mn the dopant occurs as 2+, 3+ and 4+, which indicates that it is hard to incorporate the transition metal ion in one valency.

CONCLUSION

In $GdAlO_3$ the trapping by activator ions, after excitation in the ^6I levels of Gd^{3+}, has the highest efficiency if allowed absorption bands of the activator ion overlap with the ^6I or ^6P levels of Gd^{3+}. In this case the trapping is governed by multipolar interaction. In the case of rare earth ions, these conditions are rarely fulfilled and trapping is governed by exchange interaction. The magnitudes of the several transfer rates has been estimated.

REFERENCES

1 G. Blasse, *Recl. Trav. Chim. Pays-Bas, 105* (1986) 143.

2 G. Blasse, *J. Less-Common Metals, 112* (1985) 1.

3 C.T. Garapon, B. Jacquier, J.P. Chaminade and C. Fouassier, *J. Lum., 34* (1985) 211.

4 J.Th.W. de Hair, *J. Lum., 18/19* (1979) 797.

5 Hao Zhiran and G. Blasse, *Mat. Chem. Phys., 12* (1985) 257.

6 A.J. de Vries and G. Blasse, *Mat. Res. Bull., 21* (1986) 683.

7 H.S. Kiliaan, A. Meijerink and G. Blasse, *J. Lum., 35* (1986) 155.

8 A.J. de Vries, H.S. Kiliaan and G. Blasse, *J. Solid State Chem., 65* (1986) 190.

9 R.W.G. Wyckoff, *Crystal Structures, Vol.II*, J.B. Wiley, New York, 1963.

10 H.E. Hoefdraad, *J. Solid State Chem., 15* (1975) 175.

11 A.J. de Vries and G. Blasse, *J. Physique, C10 suppl. C7* (1985) 109.

12 H.S. Kiliaan *et al*. to be published.

13 W.T. Carnall, P.R. Fields and K. Rajnak, *J. Chem. Phys., 49* (1968) 4412.

14 J.M.F. van Dijk and M.F.H. Schuurmans, *J. Chem. Phys., 78* (1983) 5317.

15 G. Blasse, G.P.M. van den Heuvel and T. van Dijk, *Chem. Phys. Letters, 62* (1979) 100.

16 M.J.J. Lammers and G. Blasse, *Mat. Res. Bull., 19* (1984) 759.

17 See e.g. C.K. Jørgensen, *Absorption spectra and chemical bonding*, Pergamon Press, Oxford, 1962.

18 J.W. Severin and G. Blasse, unpublished results.

19 M.J.J. Lammers, A. Saakes, G. Blasse and L.H. Brixner, *Mat. Res. Bull., 21* (1986) 295.

20 A. Broese van Groenou, P.F. Bongers and A.L. Stuyts, *Mater. Sci. Eng., 3* (1968/1969) 317.

21 W.T. Carnall, in K.A. Gschneider, Jr. and L. Eyring (eds), *Handbook on the Physics and Chemistry of the Rare Earths*, North Holland, Amsterdam, 1979 chap. 24.

22 T. Abritta, F. de Souza Barros and N.T. Melamed, *J. Lum., 33* (1985) 141.

23 E.W.J.L. Oomen, K. van der Vlist, W.M.A. Smit and G. Blasse, *Chem. Phys. Lett., 129* (1986) 9.

24 A. van Die, A.C.H.I. Leenaers, G. Blasse and W.F. van der Weg, to be published.